

Nuclear quadrupole alignment of $^{176}\text{Lu}^m$ and ^{177}Lu in a lutetium single crystal at low temperatures and systematics of electric field gradients in pure hexagonal transition metals

H. Ernst, E. Hagn, and E. Zech

Physik-Department, Technische Universität München, D-8046 Garching, West Germany

G. Eska

Institut für Tieftemperaturforschung, D-8046 Garching, West Germany

(Received 17 November 1978)

The quadrupole frequencies for $^{176}\text{Lu}^m$ and ^{177}Lu nuclei in a Lu single crystal have been determined by nuclear orientation at temperatures down to 6 mK as $-128(16)$ MHz and $+294(37)$ MHz, respectively. From the observed γ anisotropies several γ -ray multipole mixing ratios could be derived. With the known ground-state quadrupole moment of $Q = 3.39(2)b$ for ^{177}Lu the electric field gradient of LuLu is found to be $+3.6(5) \times 10^{17}$ V/cm². This value does not fit into the frame of Raghavan's universal correlation. Taking into account recent data on other systems, a new classification of electric field gradients in hexagonal metals is proposed: The electronic contribution to the total electric field gradient is proportional to the ionic part, the proportionality constant being *positive* for all group-IIIb and -IVb hexagonal metals and *negative* for all group-IIb, -VIIb, and -VIIIb metals.

I. INTRODUCTION

In recent years the study of nuclear quadrupole interactions in noncubic metals has gained considerable interest. From the measured quadrupole splitting $\Delta E_Q = h\nu_Q = e^2qQ$, either the electric field gradient (EFG) eq or the nuclear quadrupole moment Q can be determined if the other quantity is known. Most experiments were done to get a better understanding of the EFG in noncubic metals. The theoretical description of EFG's has been performed successfully only in few cases of simple nontransition metals such as Be, Mg, Zn, and Cd.¹ The EFG data for transition metals cannot be described theoretically at present. Two phenomenological models, however, exist, with which the observed systematics can be explained: Raghavan *et al.*² propose a relation between the electronic and ionic contributions to the EFG, which is described by a universal curve. Nishiyama and Riegel³ calculate both electronic and ionic contributions from a screened potential taking lattice vibrations into account. For the test and an eventual refinement of these models a large amount of data on EFG's in pure metals and at impurity sites is desirable. Both the sign and the magnitude are of interest. As most of the data are gained with perturbed-angular-correlation techniques, the sign determination is lacking in many cases. Most of the presently known signs have been determined by β - γ angular correlation or Mössbauer-effect measurements. These methods are applicable only to the few elements where suited isotopes exist. With the low-temperature nuclear-orientation technique (NO), the

magnitude *and* the sign can be measured, the sign determination being unambiguous, as the sign of the observed γ anisotropy depends on it directly. Moreover, there are many elements for which no isotope with a convenient, i.e., suitable long-lived, "angular correlation state," and no Mössbauer isotope exists. The NO technique, however, is applicable to all radioactive isotopes with ground-state spin $j \geq 1$ and a half-life of at least several hours. One complicating fact is that single crystals have to be used. This may be one of the reasons why only a few quadrupole NO experiments have been performed up to now.⁴⁻¹⁰ Most of these experiments were done on pure systems which were obtained by neutron irradiation of the single crystals. Only few selected systems are obtainable in this way. Using charged-particle reactions as (d, xn) , (α, xn) , or (heavy ion, xn), a large number of neutron-deficient isotopes can be produced selectively, which allows the determination of EFG's for different impurity nuclei and also the determination of ground-state quadrupole moments of many radioactive nuclei. Especially well suited for this purpose are Os and Re single crystals because of their relatively large EFG's at the impurity site, and because they have the good mechanical and thermal properties which are necessary for NO experiments. For an extension of such experiments to the heavy-rare-earth region, the use of Lu single crystals would be attractive. In a first NO experiment on $^{177}\text{LuLu}$,⁷ however, a relatively small value for the EFG of

$$eq = +1.08(4) \times 10^{17} \text{ V/cm}^2$$

was found, which does not fit into the systematics of

EFG's. In order to clarify whether this discrepancy is real, a carefully performed NO experiment seemed to be necessary.

II. NUCLEAR ORIENTATION

The angular distribution of γ rays emitted in the decay of radioactive nuclei is most conveniently written as follows¹¹:

$$W(\theta) = \sum_k B_k(\nu_Q, T) U_k F_k P_k(\cos\theta) Q_k \quad (1)$$

Generally only the $k=2$ and $k=4$ terms contribute. The orientation parameters B_k describe the degree of orientation of the initial nuclear state. They depend on the temperature T and on the energy splitting of the m substates, which, in the present case of pure axially symmetric quadrupole interaction, is given by

$$E(m) = \frac{h\nu_Q}{4j(2j-1)} [3m^2 - j(j+1)] \quad (2)$$

The quadrupole interaction frequency ν_Q is connected with the electric field gradient eq and the nuclear quadrupole moment Q ,

$$\nu_Q = e^2qQ/h \quad (3)$$

A considerable degree of orientation is obtained only if $h\nu_Q > kT$, i.e., for $eq \sim 10^{17}$ V/cm² and $Q \sim 1b$, temperatures in the region of $T \sim 10$ mK are necessary. The sign of the B_k parameters depends directly on the sign of ν_Q . This can easily be understood when viewing the extreme low-temperature limit, i.e., complete orientation. In the case of $\nu_Q > 0$, only the $m = \pm \frac{1}{2}$ states are occupied for half-integer spin (or the $m=0$ state for integer spin). This means that the orientation is "perpendicular" to the quantization direction, which is given by the c axis of the single crystal. For $\nu_Q < 0$, the $m = \pm j$ states are occupied, which forces the orientation to be collinear with the c axis. As these two configurations differ by a kind of rotation of $\frac{1}{2}\pi$, the corresponding B_2 terms must change sign. (The corresponding B_4 terms, however, have the same sign). This feature has another decisive consequence for the temperature dependence of $W(\theta)$ in the high-temperature region ($kT > h\nu_Q$), where $B_2(h\nu_Q/kT)$ can be expanded in powers of $h\nu_Q/kT$, which yields

$$B_2 \propto h\nu_Q/kT \quad (4)$$

It means that the anisotropy depends linearly on $1/T$, the slope being proportional to the quadrupole frequency ν_Q . This is in contrast to the case of the magnetic splitting, where B_2 starts with $(h\nu_M/kT)^2$.

The U_k and F_k parameters in formula (1) depend on the characteristics of the nuclear decay, i.e., on

spins, multipole orders and mixing ratios δ of different multipole orders if the nuclear transitions are not pure. As most spins in the decay sequences of "long-lived" radioactive nuclei are known, the uncertainties in the δ 's cause the largest uncertainty in the calculation of the F_k coefficients. As δ directly influences the value of the slope of $W(\theta)$ vs $1/T$, ν_Q and δ cannot be determined simultaneously in the quadrupole case, although it would be possible to do so if one could extend the measurements to such low temperatures that the anisotropy gets saturated. However, such temperatures ($T \ll 1$ mK) are not obtainable at the present state of low-temperature technology. Therefore, either only pure γ transitions or such γ transitions for which δ is known with sufficient accuracy, can be used for the determination of ν_Q . The same arguments hold, of course, for the mixing ratios of different tensor ranks in the preceding β transitions, the deorienting effect of which is taken into account by the U_k coefficients. Tables of U_k and F_k are given in Ref. 12. The $P_k(\cos\theta)$ in formula (1) are Legendre polynomials, and the Q_k coefficients are dependent on the experimental setup, as they take into account the solid angle of the detectors. To eliminate a large number of experimental uncertainties such as the decrease of the counting rates due to the depletion of the parent nuclear state, the ratio ϵ of the anisotropies measured under $\theta=0^\circ$ and $\theta=90^\circ$ with regard to the crystal c axis,

$$\epsilon = \frac{W(0)}{W(90)} - 1 \quad (5)$$

is determined and evaluated as a function of T . It is usually also called the anisotropy.

III. EXPERIMENTAL DETAILS

The sample was prepared in the following way: From a lutetium single-crystal rod purchased from Ames Lab., Iowa, U.S.A., a disk of about 5-mm diameter and a thickness of 90 μm was spark cut, with the crystal c axis being oriented perpendicularly to the disk plane. The sample was irradiated at the Munich research reactor, FRM, for 10 seconds in a neutron flux $\phi = 8 \times 10^{12}$ n/cm²sec to produce the radioactive isotopes $^{176}\text{Lu}^m$ ($T_{1/2} = 3.7$ h; $j^\pi = 1^-$) and ^{177}Lu ($T_{1/2} = 6.7$ day; $j^\pi = \frac{1}{2}^+$). After the irradiation both sides of the crystal were polished and then immediately tinned ultrasonically with Ga-In, a eutectic alloy with the low melting point of 15 $^\circ\text{C}$. It was soldered to one side of the cold finger of the cryostat. For thermometry a $^{54}\text{MnFe}$ foil was soldered to the other side of the cold finger. A second thermometer, $^{57}\text{CoNi}$, was soldered to the outer side of the Lu crystal. This setup is shown in the inset of Fig. 1. Such

a complicated arrangement is necessary, since a good thermal contact between the Lu crystal and the cold finger is one of the essential requirements in these experiments, and this can be detected by comparing the temperatures of the two thermometers. That such precautions were necessary can be seen from the fact that attempts to use In instead of Ga-In as soldering material were not successful. The sources were cooled to temperatures as low as 6 mK with a two-stage demagnetization cryostat, the details of which are described in Ref. 13. The first stage operates with Cr-K-alum as cooling salt and obtains a final temperature of 12 mK. The second stage works on the basis of hyperfine enhanced nuclear cooling. With PrCu₆ as cooling material, final temperatures of 2-3 mK can be obtained with weak radioactive sources. The relatively high final temperature of 6 mK in this experiment is probably due to radioactive heating. Because of the short half-life of ¹⁷⁶Lu^m, the relatively high activities at the start of the experiment of 50 μCi for ¹⁷⁶Lu^m and 10 μCi for ¹⁷⁷Lu had to be used. To align the ferromagnetic domains and thus to establish a unique direction of the hyperfine field of the thermometer foils, an external magnetic field of 4.5 kG was applied. During the warm-up of the cryostat from 6 to 30 mK γ spectra were measured with two coaxial Ge(Li) detectors, which were placed at 0° and at 90° with respect to the *c* axis of the single crystal.

Every 1000 seconds the spectra were written on to magnetic tape which was controlled by a PDP8E computer. For normalization, spectra were recorded at He temperature before and after every cooling run. The final analysis was done on a PDP10 computer, using Gaussian peak fitting routines.

IV. TEMPERATURE DETERMINATION

The surface temperature of the Lu crystal was determined using the ⁵⁷CoNi thermometer foil by analyzing the anisotropy of the 122- and the 136-keV γ transitions which follow the electron capture decay of ⁵⁷Co. Both anisotropies yielded the same temperature. The temperature of the cold finger was calculated from the anisotropy of the 835-keV γ rays emitted from the ⁵⁴MnFe thermometer foil. Figure 1 shows the inverse temperature measured with ⁵⁷CoNi versus that measured with ⁵⁴MnFe. In the absence of temperature gradients, the two temperatures should be equal, i.e., the measured points should be distributed around the dotted line in Fig. 1. It is clear that, especially towards lower temperatures, the deviations from the ideal curve become significant. The maximum deviation is about 20%, which means that a temperature gradient between the cold finger and the Lu crystal has to be taken into account in the determination of the overall temperature of the Lu

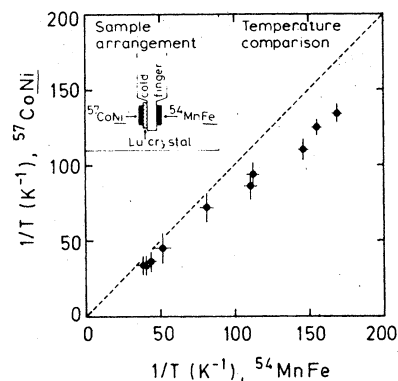


FIG. 1. Comparison of the reciprocal temperature derived from the ⁵⁷CoNi and ⁵⁴MnFe thermometers. The dashed line holds for the ideal situation that both temperatures are equal.

crystal. Two phenomena may be responsible for this gradient:

First, there may exist a large thermal-contact resistance between the cold finger and the Lu crystal due to incomplete soldering. This is supported by the fact that it is impossible to solder Lu without the use of an ultrasonic device. The surface oxide layer may be destroyed only partly by the ultrasonic tinning, so that the effective area over which the heat transport takes place may be significantly smaller than the about 20-mm² geometric area of the sample. The same effect may also be present at the contact between the Lu crystal and the ⁵⁷CoNi thermometer foil. Since the radioactive heating of ~10 μCi ⁵⁷Co in the Ni foil is smaller than that of the Lu activities in the Lu crystal, the temperature gradient between these two sources should be smaller than that between the Lu crystal and the Cu cold finger. It may, however, be of the same order of magnitude due to the extra heating caused by the β particles which are emitted from the surface layer of the Lu crystal and absorbed in the ⁵⁷CoNi thermometer.

Another effect which might be responsible for the temperature gradient is that the thermal conductivity of Lu could become small at very low temperatures. No experimental data are available for this temperature region, but at *T* ~ 1 K the experimental thermal conductivity of Lu is, by a factor of ~10, smaller than that of Re or Os.¹⁴ We have performed similar quadrupole NO experiments with ⁸Re and ¹⁰Os single crystals, the experimental setup and the soldering technique being the same, and no temperature gradients were observed in these experiments, even at the lower final temperatures of ~3 mK. Thus, it is reasonable to adopt the mean value of the two thermometers as the average temperature of the Lu crystal. The estimate of the error in this temperature has been done in such a way as to overlap both single values.

Two more effects have to be considered in the context of a correct temperature assignment: The influence of the spin-lattice relaxation and the warm-up of the sources during the measurement of one spectrum. The heat transfer between the nuclear-spin system and the lattice, i.e., the crystal, takes place via the spin-lattice relaxation mechanism. In the high-temperature region, $kT > h\nu_Q$, there is an exponential equilibration of the reciprocal temperatures, the time constant being the spin-lattice relaxation time T_1 , which follows the Korringa relation: $T_1 T = \text{const.}$ In the low-temperature region, $kT < h\nu_Q$, the relaxation process can generally not be described by one unique time constant, and the Korringa relation does not hold, either. Nevertheless, there exists a characteristic time constant T_1' , with which, in a fairly good approximation, the γ anisotropy relaxes towards the equilibrium value. If T_1' is comparable to, or even larger than, that time during which one spectrum is accumulated care has to be taken in doing the temperature assignment. An estimate of T_1' can be made by observing the time dependence of the γ anisotropies after the demagnetization.

No obvious time lag could be detected for the anisotropies of the thermometers and the anisotropies of lutetium in this experiment. Thus we conclude that spin-lattice relaxation effects can be neglected for the interpretation of the $^{176}\text{Lu}^m\text{Lu}$, $^{177}\text{LuLu}$ γ anisotropies.

Next, the warm-up effect after the demagnetization has to be considered. In the case of a warm-up from T_a to T_b , the measured γ anisotropy is given by

$$\bar{\epsilon} = \int_{1/T_a}^{1/T_b} \epsilon(1/T) p(1/T) d(1/T) \quad (6)$$

where $p(1/T)$ describes the temperature increase. As the averaging strongly depends on the structure of ϵ vs $1/T$, which is generally not the same for different systems, systematic deviations can occur if the

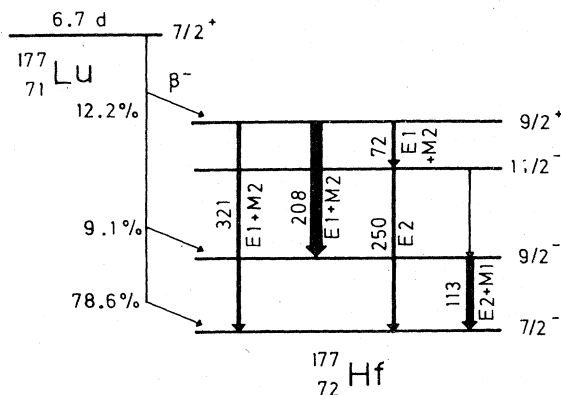


FIG. 2. Decay of ^{177}Lu to levels of ^{177}Hf .

temperature change during the accumulation of one spectrum becomes too large. We have estimated the maximal error arising from this effect under the assumption of a realistic temperature increase and found that it can be neglected in comparison to the relatively large error caused by the temperature difference between the two thermometers.

V. RESULTS

A. $^{177}\text{LuLu}$

We have measured the γ anisotropies of the 113-, 208-, 250-, and the 321-keV γ transitions as a function of the temperature. A simplified decay scheme of ^{177}Lu is shown in Fig. 2. The 250-keV γ transition is the only one with pure multipolarity. Though its γ intensity is relatively weak, it is best suited for the determination of the quadrupole splitting as all nuclear parameters involved in this decay cascade are known. The preceding β decay is allowed, thus the U_k^β coefficients are fixed by the rank-1 tensor. The multipolarity of the unobserved 72-keV γ transition is predominantly $E1$ with a small $M2$ admixture. The mixing ratio has been determined by Krane *et al.*¹⁵ as $\delta(72) = -0.051(37)$. The resulting uncertainty in the U_k coefficients is negligibly small, as only δ^2 terms enter into the calculation. Thus the quadrupole splitting is the only unknown parameter. Figure 3 shows the measured anisotropy versus $1/T$. From a least-squares fit using Eqs. (1), (2), (3), and (5) (solid line in Fig. 3), $\nu_Q = +294(37)$ MHz is found with the temperature error taken into account. The anisotropy of the 208-keV γ transition, which is shown in the upper part of Fig. 4, depends on two parameters, the $M2/E1$ multipole mixing ratio $\delta(208)$ and the quadrupole frequency ν_Q . Taking the above result for ν_Q , the least-squares fit yields $\delta(208) = +0.08(4)$. The 113-keV γ anisotropy is

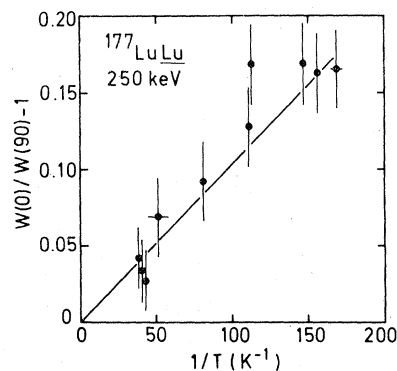


FIG. 3. Anisotropy of the 250-keV γ transition vs $1/T$ derived from the $^{54}\text{MnFe}$ thermometer.

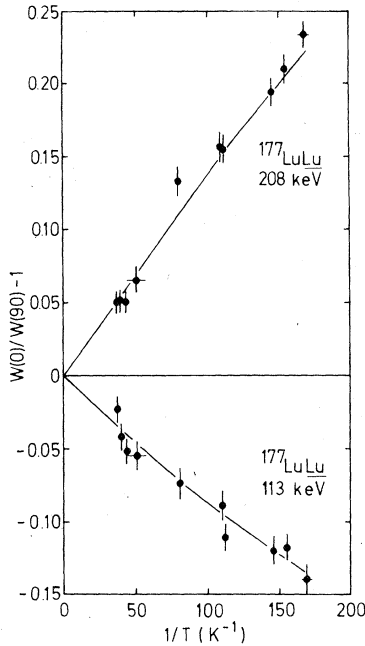


FIG. 4. Anisotropy of the 208- and the 113-keV γ transitions vs $1/T$ derived from the $^{54}\text{MnFe}$ thermometer.

shown in the lower part of Fig. 4. It depends on three parameters: the quadrupole frequency ν_Q , the $E2/M1$ multipole mixing ratio $\delta(113)$, and the rank-2 tensor to rank-1 tensor mixture Δ_β of the β decay to the $\frac{9}{2}^-$ level. From the relative β intensities of Ref. 16 and the anisotropy data of Krane *et al.*,¹⁵ one can conclude that this β transition is essentially of rank-1 tensor. Taking our value for ν_Q and $\Delta_\beta^2=0$, we get $\delta(113) = -4.7(3)$.

The anisotropy of the 321-keV γ transition is only $\epsilon = +0.023(12)$ at 6 mK. This is due to the fact that the $M2/E1$ multipole mixing ratio $\delta(321)$ causes an almost complete cancellation of the F_2 coefficient in this special case, which means that $\delta(321)$ can be determined very accurately. We find

$\delta(321) = +0.18(1)$. It should be noted that the large temperature uncertainty has a negligibly small influence in the determination of the mixing ratios. This is due to the fact that ratios of anisotropies, from which the δ 's can be determined, are nearly temperature independent. [Such ratios are *entirely* temperature independent as long as the $k=4$ terms in Eq. (1) can be neglected, i.e., in the "high-temperature" case, or if the $k=4$ terms are zero because of angular momentum reasons.]

All γ -ray mixing ratios which have been obtained are summarized, together with some previous results, in Table I. The 113-keV $E2/M1$ mixing ratio is in good agreement with other measurements. The discrepancy in the sign of the 208-keV $M2/E1$ mixing ratio has been clarified; it is positive. All mixing ratios reported here are given using the convention of Krane and Steffen.¹⁷

B. $^{176}\text{Lu}^m \text{Lu}$

The decay scheme of $^{176}\text{Lu}^m$ is shown in Fig. 5. The $2^+ \rightarrow 0^+$ γ transition has pure multipolarity $E2$, but the tensor rank of the preceding β decay is not known. Thus the quadrupole frequency and the mixing ratio Δ_β of rank-2 tensor to rank-1 tensor of the β decay determine the anisotropy. In this case only $W(0)$, which is shown in Fig. 6, could be analyzed because of experimental problems connected with the strong absorption of the 88-keV γ rays in the 90° direction. As the ratio of the quadrupole moments of $^{176}\text{Lu}^m$ and ^{177}Lu is known to be $Q(^{176}\text{Lu}^m)/Q(^{177}\text{Lu}) = -0.434(9)$ (see Sec. VIA), the quadrupole frequency for $^{176}\text{Lu}^m \text{Lu}$ is calculated as $\nu_Q = -128(16)$ MHz. Taking this into account we find $\Delta_\beta^2 \ll 0.11$ for the rank-2 tensor admixture in the β decay. This value is in good agreement with the work of van der Werf,¹⁸ who has measured shape factors of the $1^- \rightarrow 2^+$ and the $1^- \rightarrow 0^+$ β transitions and the β - γ angular correlation.

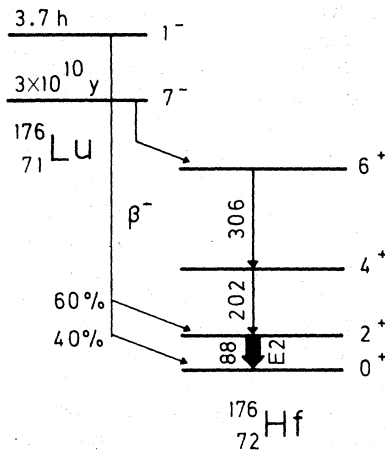
TABLE I. Mixing ratios of ^{177}Hf γ rays.

$J_i^\pi \rightarrow J_f^\pi$	L'/L	E_γ (keV)	mixing ratios			
			this work	Ref. a	Ref. b	Ref. c
$\frac{9}{2}^- \rightarrow \frac{7}{2}^-$	$E2/M1$	113	-4.7(3)	-4.7(2)	-4.65(20)	-5.45(30)
$\frac{9}{2}^+ \rightarrow \frac{9}{2}^-$	$M2/E1$	208	+0.08(4)	+0.07(2)	-0.08(2)	...
$\frac{9}{2}^+ \rightarrow \frac{7}{2}^-$	$M2/E1$	321	+0.18(1)	+0.17(1)

^aK. S. Krane, C. E. Olsen, and W. A. Steyert, Phys. Rev. C **10**, 825 (1974).

^bH. E. Keus and W. J. Huiskamp, Physica (Utrecht) B **85**, 137 (1977).

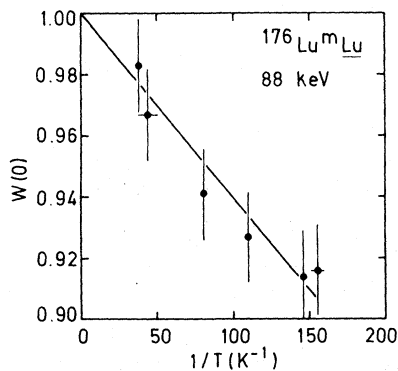
^cW. D. Brewer and G. Kaindl, Hyperfine Int. **4**, 576 (1978).

FIG. 5. Decay of $^{176}\text{Lu}^m$ to levels of ^{176}Hf .

VI. DISCUSSION

A. Quadrupole splitting of $^{177}\text{LuLu}$

The quadrupole frequency has been determined as $\nu_Q = +294(37)$ MHz. This value is significantly higher than that of Brewer and Kaindl,⁷ who found $\nu_Q = +144.3(6.0)$ MHz. This large discrepancy can most probably be ascribed to the fact that it is difficult to establish a good thermal contact between Lu and the cold finger because of the poor soldering properties of Lu. With an imperfect thermal contact, a large temperature gradient may be present between the Lu crystal and the cold finger, which may lead to a misinterpretation of the γ anisotropy, and thus to a too small value for ν_Q , if only the temperature of the cold finger is measured.

FIG. 6. Counting rate $W(0)$ of the 88-keV γ transition vs $1/T$ derived from the $^{54}\text{MnFe}$ thermometer.

There are several other effects such as lattice imperfections or radiation damage due to the neutron irradiation which could influence the value of the γ anisotropy. The corresponding uncertainty in ν_Q is assumed to be small in comparison to the quoted error for ν_Q . This is supported by the results of time-differential perturbed-angular-correlation (TDPAC) measurements on Hf single crystals.¹⁹ Furthermore, we have performed quadrupole NO experiments on $^{186,188}\text{ReRe}$ and $^{191}\text{OsOs}$. No significant variation of ν_Q has been found if the annealing step after the irradiation had been omitted.

To determine the electric field gradient eq from our measured quadrupole frequency ν_Q , a reliable value for the nuclear quadrupole moment has to be available. Peterson and Shugart²⁰ have analyzed the hyperfine structure of ^{177}Lu in the $^2D_{3/2}$ ground state and in the $^2D_{5/2}$ electronic state using the atomic-beam magnetic-resonance technique and have reported a value for the quadrupole moment:

$$Q^{\text{AB}}(^{177}\text{Lu}) = +5.51(6) \text{ b} .$$

Similar experiments have been performed on the stable isotope ^{175}Lu and on the radioactive isotope $^{176}\text{Lu}^m$ ($T_{1/2} = 3.7\text{h}$), with results^{21,22}

$$Q^{\text{AB}}(^{175}\text{Lu}) = +5.68(6) \text{ b} ,$$

and

$$Q^{\text{AB}}(^{176}\text{Lu}^m) = -2.39(4) \text{ b} .$$

There is, however, a fundamental uncertainty in the determination of quadrupole moments from this type of experiments. From the measured energy splittings of the hyperfine F states, the quantity B is derived, which contains the product of Q times the electric field gradient of the free atom eq^{fa} , and therefore, for the determination of Q^{AB} , eq^{fa} has to be calculated. Especially for high- Z systems, these calculations may contain severe uncertainties.

Another method for the determination of ground-state quadrupole moments of stable nuclei is the x-ray spectroscopy of muonic atoms. It is based on the observation of the quadrupole splitting of the excited states of the cascade in muonic atoms for which the splitting is large enough to be observed and at the same time the point-nucleus approximation is valid. As the field gradient of the muon is precisely known, Q can be determined reliably. Dey *et al.*²³ have applied this technique to muonic ^{175}Lu , and found $Q^{\text{MU}} = +3.49(2)$ b, which is significantly smaller than the atomic-beam value. If one attributes this difference to an incorrect free-atom field gradient, all Lu quadrupole moments which have been determined with the atomic-beam technique should be renormalized by the factor

$$Q^{\text{MU}}(^{175}\text{Lu})/Q^{\text{AB}}(^{175}\text{Lu}) .$$

This renormalization of the quadrupole moments towards smaller values is supported by Coulomb excitation data,²⁴ from which $Q(^{175}\text{Lu}) = +3.5(1)$ b and $Q(^{177}\text{Lu}) = +2.5(3)$ b would be expected. These data are all compiled in Table II. The renormalization yields $Q(^{177}\text{Lu}) = +3.39(2)$ b, which can now be used to deduce the electric-field gradient of LuLu from our measurement. The result is

$$eq = +3.6(5) \times 10^{17} \text{ V/cm}^2,$$

which is discussed in Sec. VI B.

B. Electric field gradient of LuLu

The description of EFG's in metals has traditionally been done in the framework of Eq. (7),²⁵

$$eq = eq_{\text{latt}}(1 - \gamma_{\infty}) + eq_{\text{el}}, \quad (7)$$

where γ_{∞} is the Sternheimer antishielding factor. The ionic part, $eq_{\text{ion}} = eq_{\text{latt}}(1 - \gamma_{\infty})$, can easily be calculated using lattice sum methods.^{26,27} The calculation of the electronic gradient eq_{el} , however, is complicated; it has been performed only in a few cases, the results being not very encouraging up to now. Raghavan *et al.*² compiled a lot of data on EFG's and found an experimental trend which is described by the empirical relation

$$eq_{\text{el}} = -K eq_{\text{latt}}(1 - \gamma_{\infty}), \quad (8)$$

where K is a positive constant of the order of three. The total EFG can then be written as follows:

$$eq = eq_{\text{latt}}(1 - \gamma_{\infty})(1 - K) + e\bar{q}, \quad (9)$$

where $e\bar{q}$ accounts for small individual deviations which are described in detail in Ref. 2. This correlation means that eq_{el} and the total EFG, eq , are opposite in sign to eq_{latt} . In the case of LuLu

$$eq_{\text{ion}} = +1.36 \times 10^{17} \text{ V/cm}^2$$

is calculated. Thus one would expect

$$eq = -2.8 \times 10^{17} \text{ V/cm}^2$$

from the relation of Raghavan *et al.*, in contradiction to our experimental value of

$$eq = +3.6(5) \times 10^{17} \text{ V/cm}^2,$$

which has the right magnitude, but the opposite sign. We will show, however, that this result does not represent an exception, but fits well into a systematics of EFG's of hexagonal transition metals. To do that we discuss the EFG's in a similar manner as done by Raghavan *et al.*, but in a smaller frame. At the present stage we confine the discussion to pure systems of hexagonal transition elements, including the rare-earth metals. This is reasonable for the beginning, as the EFG's of impurity systems and of systems with different crystal structures show deviations from the main trend, which is extensively outlined in Ref. 2. All EFG data available on pure hexagonal systems have been compiled in Table III, together with calculated values for eq_{ion} and the values for eq_{el} which are given by $eq_{\text{exp}} - eq_{\text{ion}}$. The ionic field gradients have been calculated according to

$$eq_{\text{latt}} = (Ze/a^3)[0.0065 - 4.3584(c/a - 1.6330)], \quad (10)$$

TABLE II. Quadrupole moments of ^{175}Lu , $^{176}\text{Lu}^m$, and ^{177}Lu .

Nucleus	J^{π}	Nilsson state	Quadrupole moments [b]			
			Q^{MU}	Q^{AB}	Q^{CE}	Renormalized
^{175}Lu	$\frac{7}{2}^{+}$	$p 7/2 [404]$	+3.49(2) ^a	+5.68(6) ^b	+3.5(1) ^e	+3.49(2)
$^{176}\text{Lu}^m$	1^{-}	$p 7/2 [404] n 7/2 [514]$...	-2.39(4) ^c	...	-1.47(1)
^{177}Lu	$\frac{7}{2}^{+}$	$p 7/2 [404]$...	+5.51(6) ^d	+2.5(3) ^e	+3.39(2)

MU: x-ray spectroscopy of muonic atoms

AB: Atomic beam

CE: Coulomb excitation

^aW. Dey, P. Ebersold, H. J. Leisi, F. Scheck, H. K. Walter, and A. Zehnder (to be published); cited in: P. Ebersold *et al.*, Nucl. Phys. A **296**, 493 (1978). The less precise value $Q = 3.50 \pm 0.07$ b is given in: W. Dey, P. Ebersold, H. J. Leisi, F. Scheck, H. K. Walter, and A. Zehnder, Helv. Phys. Acta. **47**, 93 (1974).

^bG. J. Ritter, Phys. Rev. **126**, 240 (1962).

^cM. B. White, S. S. Alpert, S. Penselin, T. I. Moran, V. W. Cohen, and E. Lipworth, Phys. Rev. **137**, B477 (1965).

^dF. R. Petersen and H. A. Shugart, Phys. Rev. **126**, 252 (1962).

^eK. E. G. Löbner, M. Vetter, and V. Hönig, Nucl. Data Tables A **7**, 495 (1970).

TABLE III. Systematics of electric field gradients in pure hexagonal group II*b*, III*b* (including the rare earths), IV*b*, VII*b*, and VIII*b* metals. The experimental EFG data eq_{exp} , the ionic contribution $eq_{\text{ion}} = eq_{\text{latt}}(1 - \gamma_{\infty})$, and the electronic part $eq_{\text{el}} = eq_{\text{exp}} - eq_{\text{ion}}$ are listed. All numbers are given in units of 10^{17} V/cm². Predicted signs for eq_{exp} , whose signs have not been measured, and the corresponding values for eq_{el} are put in parentheses. The experiments on Cd, Sc, Tc, and Ru have been performed at room temperature, all others at low temperatures. The structure of La is not simple hcp, but dhcp, which means that the layer sequency is *ABCABC* instead of *ABAB*. Therefore two inequivalent lattice sites with eq_{latt} differing by 10% should exist. In the cases of Tb, Dy, and Tm, it should be noted that eq_{exp} is the measured EFG minus the calculated contribution of the unfilled 4*f* shell. Therefore these values are possibly of less significance.

Group	lattice ^a	eq_{exp}	eq_{ion}	eq_{el}
II <i>b</i>	Zn	+3.0(2)	-1.96	+5.0
	Cd	+6.7(9)	-3.63	+10.3
	Cd (24 kbar)	+6.0(9)	-2.90	+8.9
	Cd (50 kbar)	+5.4(8)	-2.60	+8.0
	Cd (74 kbar)	+4.8(8)	-2.50	+7.3
III <i>b</i>	Sc	(+)0.38(2)	+0.22	(+0.16)
	La	(+)1.5(2)	+0.50	(+1.0)
	Gd	+2.8(3)	+1.06	+1.7
	Tb	+3.4(1.7)	+1.32	+2.1
	Dy	+4.3(1.5)	+1.53	+2.8
	Tm	+5.0(8)	+1.64	+3.4
	Lu	+3.6(5)	+1.36	+2.2
IV <i>b</i>	Ti	(+)1.2(1)	+0.40	(+0.8)
	Hf	+9.5(4)	+2.84	+6.7
VII <i>b</i>	Tc	(-)0.7(4)	+1.56	(-2.3)
	Re	-4.9(2)	+2.08	-7.0
VIII <i>b</i>	Fe (ϵ phase)	(-)0.26(5)	+0.44	(-0.70)
	Co	-0.29(2)	+0.15	-0.44
	Ru	(-)0.49(14)	+1.41	(-1.90)
	Os	-4.5(3)	+3.24	-7.7

^aZn: W. Potzel, A. Forster and G. M. Kalvius, Phys. Lett. A 67, 421 (1978).

Cd: P. Raghavan, R. S. Raghavan, and E. N. Kaufmann, Phys. Lett. A 48, 131 (1974).

Cd under high pressure: P. Raghavan, R. S. Raghavan, and W. B. Holzapfel, Phys. Rev. Lett. 28, 903 (1972).

Ru: H. Haas and D. A. Shirley, J. Chem. Phys. 58, 3339 (1973).

Sc: R. G. Barnes, F. Borsa, S. L. Segel, and D. R. Torgeson, Phys. Rev. 137, A1828 (1965).

La: A. Narath, Phys. Rev. 179, 359 (1969).

Gd: E. R. Bauminger, A. Diamant, I. Felner, I. Nowik, and S. Ofer, Phys. Rev. Lett. 34, 962 (1975).

Tb, Dy, Tm: J. Pelzl, Z. Phys. 251, 13 (1972).

Lu: This work.

Ti: A. Narath, Phys. Rev. 162, 320 (1967).

Hf: P. Boolchand, B. L. Robinson, and S. Jha, Phys. Rev. 187, 475 (1969).

Tc: W. H. Jones and F. J. Milford, Phys. Rev. 125, 1259 (1962).

Re: Magnitude: J. Buttet, and P. K. Baily, Phys. Rev. Lett. 24, 1220 (1970). Sign: P. E.

Gregers-Hansen, M. Krusius, and G. R. Pickett, Phys. Rev. Lett. 27, 38 (1971).

Fe: D. L. Williamson, S. Bukshpan, and R. Ingalls, Phys. Rev. B 6, 4194 (1972).

Co: Magnitude: M. Kawakami, T. Hihara, Y. Koi, and T. Wakiyama, J. Phys. Soc. Jpn. 33, 1591 (1972). Sign: E. Zech, E. Hagn, H. Ernst, and G. Eska, Hyperfine Int. 4, 342 (1978).

Os: H. Ernst, W. Koch, F. E. Wagner, and E. Bucher, Phys. Lett. (to be published).

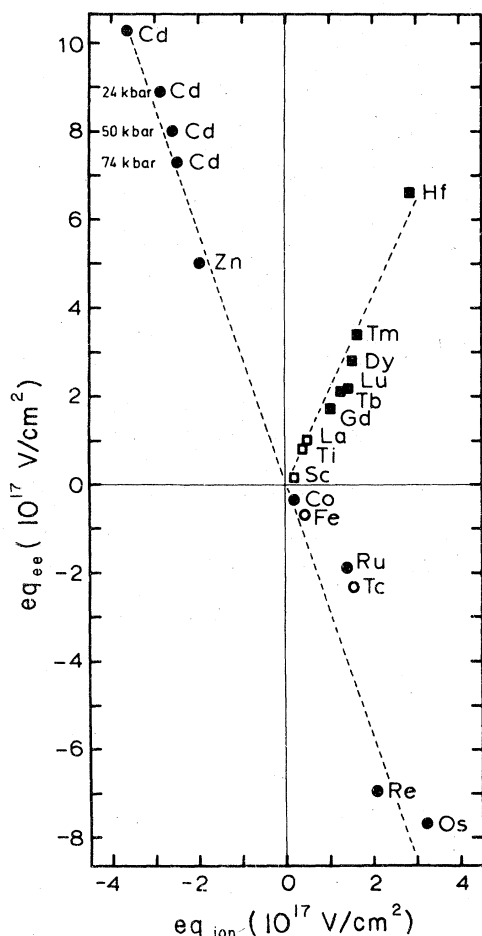


FIG. 7. Correlation of ionic and electronic contributions to the total electric field gradient in pure hexagonal metals. Circles indicate data from group-IIb, -VIIb, and -VIIIb metals, squares indicate data from group IIIb and IVb metals. Open symbols refer to data with unknown signs, their locations are predicted.

and

$$eq_{ion} = eq_{latt}(1 - \gamma_{\infty}) \quad (11)$$

[Formula 10 is valid for hexagonal-close-packed (hcp) structures with lattice constants a and c in a range for c/a which is approximately given by $1.5 \leq c/a \leq 2.0$; the latter condition is fulfilled for all hcp transition metals]. The Sternheimer factors have been taken from Refs. 28 – 30 and the lattice constants from Refs. 31 and 32. The values for Z have

been chosen in analogy to Ref. 1.

Figure 7 shows the behavior of eq_{el} vs $eq_{latt}(1 - \gamma_{\infty})$. The dotted line in quadrants II and IV represents the relationship of Raghavan *et al.*, the constant of proportionality K of Eq. (8) being $K \sim +3$. The corresponding data of the group IIIb and IVb metals are all distributed in quadrant I of Fig. 7. The dotted line represents the experimental trend and supports a proportionality between the electronic and the ionic part, the factor K of Eq. (8) being $K \sim -2$. Thus eq_{el} and eq_{ion} have the same sign for these elements, the electronic gradient being about twice the lattice gradient. No data points are expected to lie in quadrant IV. This is due to the fact that the c/a ratios of all the group IIIb and IVb metals are smaller than 1.6345, for which eq_{latt} vanishes. Thus, according to Eq. (10), only positive lattice gradients can occur for these groups.

At the present state, we cannot decide whether the proportionality holds between eq_{el} and eq_{latt} or between eq_{el} and $eq_{latt}(1 - \gamma_{\infty})$ for the data in quadrant I, as a significant variation of γ_{∞} is still lacking. Following the arguments of Raghavan *et al.*, the proportionality to $eq_{latt}(1 - \gamma_{\infty})$ can be understood as this quantity is responsible for a nonsphericity of the ionic core of the interacting nucleus which results both from the lattice gradient and from the deformability of the core. This nonsphericity influences the conduction electron cloud distributed around the central ion and thereby creates a large EFG. The novelty is that the sign and the magnitude depend on the specific electronic group. If we write

$$eq = eq_{latt}(1 - \gamma_{\infty})(1 - K) \quad (12)$$

the constant K is found to be $K \sim -2$ for the groups IIIb and IVb, where the outmost d shell is less than half-filled, and $K \sim +3$ for the groups VIIb, VIIIb, and IIb, where the d shell is half-filled, more than half-filled, or completely filled, respectively. No theoretical interpretation for this behavior can be given at present.

ACKNOWLEDGMENTS

We wish to thank Dr. T. Butz, Dr. W. Potzel, Dr. F. E. Wagner, and Dr. G. Wortmann for their help and stimulating discussions. This work was supported by the Bundesministerium für Forschung und Technologie.

¹T. P. Das, Phys. Scr. **11**, 121 (1975).

²P. Raghavan, E. N. Kaufmann, R. S. Raghavan, E. J. Ansaldo, and R. A. Naumann, Phys. Rev. B **13**, 2835 (1976).

³K. Nishiyama and D. Riegel, Hyperfine Int. **4**, 490 (1978).

⁴G. Kaindl, F. Bacon, and A. J. Soinski, Phys. Lett. B **46**, 62 (1973).

⁵S. S. Rosenblum and W. A. Steyert, Phys. Lett. A **53**, 34 (1975).

- ⁶P. Herzog, H. R. Folle, and E. Bodenstedt, *Hyperfine Int.* **3**, 361 (1977).
- ⁷W. D. Brewer and G. Kaindl, *Hyperfine Int.* **4**, 576 (1978).
- ⁸H. Ernst, E. Hagn, E. Zech, and G. Eska, *Hyperfine Int.* **4**, 581 (1978).
- ⁹P. Herzog, K. Krien, J. C. Soares, H.-R. Folle, K. Freitag, F. Reuschenbach, M. Reuschenbach, and R. Trzcinski, *Phys. Lett. A* **66**, 495 (1978).
- ¹⁰H. Ernst, E. Hagn, E. Zech, and G. Eska (unpublished).
- ¹¹S. R. de Groot, H. A. Tolhoek, and W. J. Huiskamp, in *Alpha-, Beta- and Gamma-Ray Spectroscopy*, edited by K. Siegbahn (North-Holland, Amsterdam, 1968), Vol. 2, p. 1199.
- ¹²T. Yamazaki, *Nucl. Data Sec. A* **3**, 1 (1967).
- ¹³K. Andres, E. Hagn, E. Smolic, and G. Eska, *J. Appl. Phys.* **46**, 2752 (1975).
- ¹⁴Y. S. Touloukian, R. W. Powell, C. Y. Ho, and P. G. Klemens, *Thermophysical Properties of Matter* (Plenum, New York, 1970), Vol. 1.
- ¹⁵K. S. Krane, C. E. Olsen, and W. A. Steyert, *Phys. Rev. C* **10**, 825 (1974).
- ¹⁶Y. A. Ellis and B. Harmatz, *Nucl. Data Sheets* **16**, 135 (1975).
- ¹⁷K. S. Krane and R. M. Steffen, *Phys. Rev. C* **2**, 724 (1970).
- ¹⁸S. Y. van der Werf, *Z. Phys.* **259**, 45 (1973).
- ¹⁹H. Ernst, T. Butz, and A. Vasquez, *J. Phys. F* **7**, 1329 (1977); R. L. Rasera, T. Butz, A. Vasquez, H. Ernst, G. K. Shenoy, B. D. Dunlap, R. C. Reno, and G. Schmidt, *J. Phys. F* **8**, 1579 (1978).
- ²⁰F. R. Petersen and H. A. Shugart, *Phys. Rev.* **126**, 252 (1962).
- ²¹G. J. Ritter, *Phys. Rev.* **126**, 240 (1962).
- ²²M. B. White, S. S. Alpert, S. Penselin, T. I. Moran, V. W. Cohen, and E. Lipworth, *Phys. Rev.* **137**, B477 (1965).
- ²³W. Dey, P. Ebersold, H. J. Leisi, F. Scheck, H. K. Walter, and A. Zehnder, *Helv. Phys. Acta* **47**, 93 (1974).
- ²⁴K. E. G. Löbner, M. Vetter and V. Hönig, *Nucl. Data Tables A* **7**, 495 (1970).
- ²⁵M. H. Cohen and F. Reif, in *Solid State Physics*, edited by F. Seitz and D. Turnbull (Academic, New York, 1975), Vol. 5, p. 321.
- ²⁶F. W. de Wette, *Phys. Rev.* **123**, 103 (1961).
- ²⁷T. P. Das and M. Pomerantz, *Phys. Rev.* **123**, 2070 (1961).
- ²⁸F. D. Feiock and W. R. Johnson, *Phys. Rev.* **187**, 39 (1969).
- ²⁹R. P. Gupta and S. K. Sen, *Phys. Rev. A* **7**, 850 (1973).
- ³⁰R. P. Gupta and S. K. Sen, *Phys. Rev. A* **8**, 1169 (1973).
- ³¹W. B. Pearson, *A Handbook of Lattice Spacings and Structures of Metals and Alloys* (Pergamon, London, 1967), Vol. 2, p. 80.
- ³²H. Mao, W. A. Bassett, and T. Takahashi, *J. Appl. Phys.* **38**, 272 (1967).